International Communications in Heat and Mass Transfer 136 (2022) 106195

Contents lists available at ScienceDirect

International Communications in Heat and Mass Transfer

journal homepage: www.elsevier.com/locate/ichmt

Study of tree-shaped optimized fins in a heat sink filled by solid-solid nanocomposite phase change material

Nidhal Ben Khedher [a,b], Mohammad Ghalambaz [e], Abed Saif Alghawli [c], Ahmad Hajjar [d], Mikhail Sheremet [e], S.A.M. Mehryan [f,*]

[a] Department of Mechanical Engineering, College of Engineering, University of Ha'il, 81451 Ha'il City, Saudi Arabia
[b] Laboratory of Thermal and Energetic Systems Studies (LESTE) at the National School of Engineering of Monastir, University of Monastir, Tunisia
[c] Computer Science Department, Prince Sattam Bin Abdulaziz University, 11912 Aflaj, Saudi Arabia
[d] LabECAM, ECAM Lyon, Université de Lyon, Lyon, France
[e] Laboratory on Convective Heat and Mass Transfer, Tomsk State University, 634045 Tomsk, Russia
[f] Young Researchers and Elite Club, Yasooj Branch, Islamic Azad University, Yasooj 7591493686, Iran

ARTICLE INFO

Keywords:
Tree-shaped optimized fins
Plate-fin
Solid-solid PCM
Heat sink
Nanocomposite of neopentyl glycol/CuO

ABSTRACT

The aim of this work is to comprehensively study the effect of the material of the simple plate and tree-shaped optimized fins on the thermal behavior of an enclosed medium filled with a nanocomposite of neopentyl glycol/CuO solid-solid PCM. Increasing the heat transfer rate using a fixed amount of material is an important task that improves the fin performance. The tree-shaped fin is optimized based upon the density-based structure optimization method. A transient model based upon the enthalpy method is employed to numerically study the thermal behavior of the enclosed medium containing the SS-PCM. The thermal performance of the heat sink with the tree-shaped optimized and simple plate fins made of different materials are explored. Results show that the aluminum and copper fins have the highest melting rate compared to the examined materials. Their melting rate is 50% higher than steel 302 in the case of flat plates, and 25% in the case of a tree structure. Also, the tree-shaped optimized fins outperform the plate structure fins by reaching the lowest temperature of the concentrated heat source and temperature non-uniformity under the condition that the two strucutures have the same height. When the two heights are different, the temperature distribution was optimized for materials with the lowest thermal conductivity. For steel materials, a 10% decrease in the maximum temperature was observed in the tree structure compared to the flat plates. Finally, it was shown that the nanoparticle fraction played a negligible role in heat transfer, as less than 1% change in melting rate and temperature parameters was obtained.

1. Introduction

Nowadays, phase change materials have found important applications in the thermal management of electronic components [1]. This is since many electronic components, such as portable microprocessors and power electronic devices, operate under transient workloads and produce time-dependent heat. Thus, managing transient thermal loads to keep the electronics cool is a critical issue [2]. The heatsinks filled with the phase change materials (PCM) phase change heatsinks is a promising approach for damping transient thermal loads and preventing overheating [3,4].

Phase change material, enclosed inside heatsinks, is capable of storing a notable amount of thermal energy, which can be released/stored at a constant fusion temperature. During transient high working loads, the PCM inside the heatsink melts and absorbs the excess heat of the component. Later, the PCM releases its heat and solidifies when the device works under a low working load [5]. Some recent patents utilized phase change materials for cooling electronics, such as PCM-heatsinks coupled with liquid cooling [6], PCMs coupled with refrigerants [7], a method of pouring PCMs into electronic heatsinks [8], and temperature control of batteries [9].

Although PCMs have a high capacity for storing thermal energy, they suffer from low thermal conductivity and poor heat transfer properties [10,11]. Therefore, heat transfer enhancement techniques such as using

* Corresponding author.
E-mail addresses: m.ghalambaz@gmail.com (M. Ghalambaz), a.alghauly@psau.edu.sa (A.S. Alghawli), ahmad.hajjar@ecam.fr (A. Hajjar), sheremet@math.tsu.ru (M. Sheremet), alal171366244@gmail.com (S.A.M. Mehryan).

https://doi.org/10.1016/j.icheatmasstransfer.2022.106195

Available online 24 June 2022

fins [12–14], metal foams [15–17], nano-additives [18–20], and encapsulation [21] have been applied to improve the heat transfer capabilities of PCMs.

Using thermal conductive fins is a reliable and efficient way of improving heat transfer in PCMs for long-term usage. However, the concentrated mass of fins can raise the weight and cost of the thermal storage unit since the fins do not contribute to phase change energy storage. Therefore, the shape of fins is an important design parameter that could effectively improve the heat transfer and reduce the weight and cost of a phase change heatsink. Considering the shape of fins in PCM heat sinks, there are several investigations. For example, Singh and Giri [22] examined the performance of using aluminum pin-fin configurations in a heatsink filled with eicosane. They considered four heat sink designs consisting of 40 and 56 pin fins, while a heatsink with no fins was taken as the reference. The results showed that using pin fins could significantly enhance the heat transfer. Arshad et al. [3] explored the thermal behavior of a PCM-heatsink made of plate fins where the space between the fins was filled with RT-35HC PCM to absorb the excess heat. The phase change heat transfer in the heatsink was simulated for two heatsink designs of 10% and 20% volume fraction plate-fins and fins. Fins with various heights, 10, 15, and 20 mm were examined. While the base of the heatsink was subject to a constant heat flux. Compared with a PCM filled heat sink with no fins, the results revealed that a PCM filled heatsink could decrease the heatsink's temperature and enhance the PCM melting uniformity. An increment in the volume fraction of fins and their height could reduce the heatsink temperature.

Kim et al. [23] enclosed a layer of paraffin embedded in copper foam inside a finned heatsink. They also used a layer of graphene to ameliorate the heat transfer uniformity between the composite PCM and heatsink. The results indicated that the PCM heatsink could ~~time~~ delay ~~the~~ overheating by up to ~27.3% in reduced cooling conditions. Nakhchi et al. [24] utilized stair fin types extended in the PCM enclosure to promote the heat transfer of phase change materials. They examined two configurations of stair fins mounted in either upward or downward directions on the heated wall. It was found that downward fins perform much better than upward fins due to molten PCM's natural convection effects.

The literature shows that the shape of the fins could notably change the thermal behavior and heat transfer rate of a PCM heatsink. Although inserting thermal conductive fins could significantly enhance the rate of PCM phase change and ameliorate the performance of the heatsink, the additional volume and mass of the fins are typically not desirable factors. Thus, some recent researchers have attempted to optimize the mass and shape of fins. Considering this approach, Xie et al. [25] utilized the topological optimization approach, developed by [26], to optimize the shape of fins in a PCM heatsink. The aim of the optimization approach was to find optimal heat transfer conduction paths from the heat source into the PCM regions. The optimized structure was a tree-like fin structure, which could provide enhanced melting capability compared to a plate-fin design with the same volume fraction of metals. In another study, Xie et al. [27] investigated the operating thermal behavior of tree-shaped fins in heatsinks filled with paraffin wax and under various critical temperatures. The tree shape of fins proposed by Xie et al. [25] will be utilized in the present study as an optimal shape for fins.

Solid-solid PCMs (SS-PCM) have been introduced with enhanced thermophysical properties during the past few years [28,29]. The novel SS-PCMs are beneficial in portable applications since the PCM is solid in both low energy and high energy states and does not require special care in handling liquids for typical PCMs. Therefore, SS-PCMs have attracted the attention of recent researchers. In the SS-PCM, a regular solid phase is converted to an irregular solid phase during the phase change flow. Parveen and Suresh [30] examined the possible application of neopentyl glycol (NPG)/CuO composite SS-PCM in heatsink applications. They prepared samples of composite SS-PCMs with various volume fractions of additives. They reported that using SS-PCMs could reduce the required time for the heatsink to reach a critical temperature by 2.36 times. Du et al. [31] synthesized SS-PCMs with flame retardant capability with a high energy storage density of 124.4–129.8 J/g. Raj et al. [32] proposed SS-PCMs with a high heat capacity of 73.83 J/g with stable properties of up to 1000 cycles. Such materials are promising for the development of SS-PCM heatsinks. Using SS-PCMs, Raj et al. [33] assessed the capability of SS-PCM heatsinks for cooling satellite avionics under transient thermal loads. They used pin-fins inside the heatsink to improve the heat transfer of SS-PCM. The authors examined fins with circular, square, and triangular shapes. The simulation results showed that triangular fins led to better cooling performance than other shapes.

The literature review shows that various geometrical shapes were investigated to improve heat transfer in thermal energy storage applications. However, only a few studies investigated the thermal management of SS-PCMs heatsinks for cooling electronic devices. The literature review reveals optimization techniques that could significantly promote the heat transfer potential of fins by producing complex geometrical shapes such as tree shape fins. The present study aims to utilize the optimized tree shape fins proposed in [25] and the SS-PCM material proposed in [32] and examine the optimized performance of SS-PCM heatsinks for cooling electronic components.

2. Mathematical model

A schematic view of a heat sink of the plate fins as a thermal management solution is pictured in Fig. 1(a). The plate fins are evenly spaced, and the void spaces are filled by the SS-PCM. To extract heat from an electronic device (a 1.5 cm-length concentrated heat source), a 10 cm × 10 cm enclosure saturated with a nanocomposite of neopentyl glycol/CuO solid-solid PCM is suggested. The heat source is assumed to generate a heat flow of 50 kW/m^2. (See Tables 1 and 2.)

The most widely used techniques for heat extraction from the heat generation devices through the SS-PCM are based upon heat sinks with the conventional plate-fin structure, forming a specified volume fraction of the whole enclosure. As in this heat sink, the plate fins in the enclosure are equally distributed, as shown in Fig. 1. One promising technique that ensures better heat distribution and diffusion and efficient volume management of the enclosure is a density-based topological optimization method extended by Liu and Tovar [26].

This approach ensured better heat diffusion by rebuilding the heat conduction paths and directions arising from the heat generation device into the designated PCM zone. Fig. 1(b) depicts innovative heat sinks based on topologically optimized tree shape designs. Further details on the topological optimization can be found in [26].

The fins are considered to be made of different materials, including aluminum (Al), copper (Cu), carbon steel (CS), and steel 302 (S302). The thermophysical properties of the planted fins are inserted in Table 3.

Because the specified PCM enclosure designs are symmetric, half of

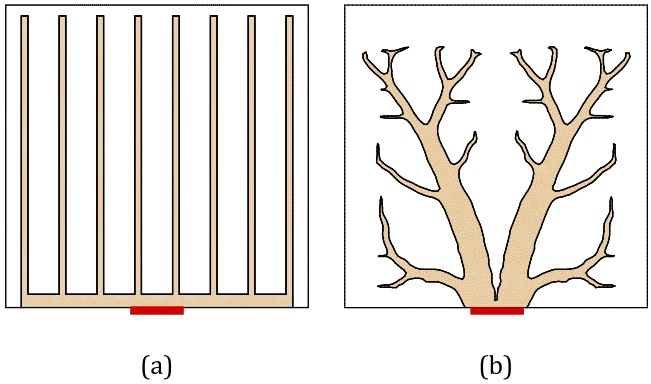

Fig. 1. (a) heat sink with plate fins design (b) heat sink with topologically optimized tree shape design.

Table 1
Thermophysical properties of the fins with different material.

Material	Al	Cu	CS	S302
Density (kg/m^3)	2710	8978	7854	8055
Specific heat capacity (J/kg K)	897	381	434	480
Thermal conductivity (W/m K)	202	387.6	60.5	15.1

Table 2
Thermophysical properties of the NPG and nano-additives [30].

Properties	Neopentyl glycol (NPG)	CuO
ρ (kgm^{-1})	1060	6500
C_p (JkgK^{-1})	1758.7	535.6
k (Wm^{-1} K^{-1})	0.12	69

Table 3
Thermo-physical properties of the composite, including CuO nano-additives [30].

Thermo-physical properties		pure	0.5 wt% CuO	1 wt% CuO	3 wt% CuO
Thermal conductivity ($Wm^{-1}K^{-1}$)		0.12	0.26	0.42	0.61
Latent heat ($kJkg^{-1}$)		124.4	120.5	118.6	112.4
SS-NPCM transition temperature ($^{\circ}C$)	Onset	40.35	39.3	39.2	39.9
	Peak	44	43.64	43.9	42.9
	End set	46.7	46.16	45.23	45.1

the domain can be addressed to reduce computational time. The 2D schematic design of the studied model as well as the boundary conditions, are shown in Fig. 2.

3. Governing equations and boundary conditions

To simulate the phase transition involving a solid-solid interface, the presented-below controlling equations are employed:

I) Energy conservation for SS-PCM [14,20]

$$(\rho C_p)_{com}\frac{\partial T}{\partial t} = \nabla.(\lambda_{com}\nabla T) - \rho_{com}h_{com}\frac{\partial \ell(T)}{\partial t} \tag{1}$$

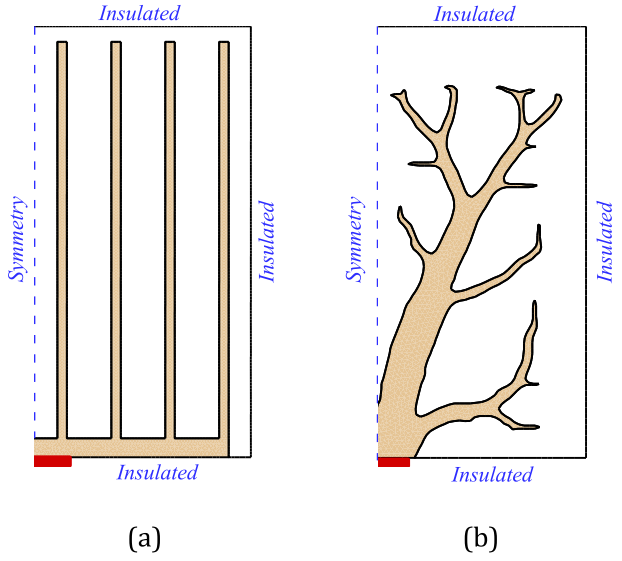

Fig. 2. The 2D schematic design of the studied model; (a) plate-fin structure and (b) tree-shaped fin structure.

$$\ell(T) = \begin{cases} 0 & T < T_{mel} - \Delta T_{mel}/2 \\ \dfrac{T - T_{mel}}{\Delta T_{mel}} + \dfrac{1}{2} & T_{mel} - \Delta T_{mel}/2 < T < T_{mel} + \Delta T_{mel}/2 \\ 1 & T > T_{mel} + \Delta T_{mel}/2 \end{cases} \tag{2}$$

$\ell(T)$ is the local volume fraction of the irregular solid phase of the SS-PCM.

II) Energy conservation for the fin [14]

$$(\rho C_p)_{fin}\frac{\partial T}{\partial t} = \nabla.(\lambda_{fin}\nabla T) \tag{3}$$

4. Controlling boundary and initial conditions

At the outer walls:

$$\left.\frac{\partial T}{\partial n}\right|_{com} = 0 \tag{4}$$

At the walls of the fins:

$$T|_{fin} = T|_{com}, \lambda_{fin}\left.\frac{\partial T}{\partial n}\right|_{fin} = \lambda_{com}\left.\frac{\partial T}{\partial n}\right|_{com} \tag{5}$$

At the root of the fins.

$$\lambda_{fin}\left.\frac{\partial T}{\partial n}\right|_{fin} = Q_f = 50000w \Big/ m^2 \tag{6}$$

The initial condition for the domain can be expressed as the following:

$$T|_{com} = T|_{fin} = T_{initial} \tag{7}$$

the volume fraction of the irregular phase of the matter is evaluated as:

$$IPF(t) = \frac{\int_{\forall}\ell(T)d\forall}{\int_{\forall}d\forall} \tag{8}$$

To calculate the density and specific heat capacity of the nano-composite, the weighted functions of the volume fraction of the nano-additives are used as follows [14]:

$$(\rho C_p)_{com} = (\rho C_p)_{PSS-PCM}(1-\phi) + (\rho C_p)_{na}\phi \tag{9}$$

$$\rho_{com} = \rho_{PSS-PCM}(1-\phi) + \rho_{na}\phi \tag{10}$$

Also, the following relationship converts the mass fraction to the volume fraction:

$$\phi = \frac{\rho_{PSS-PCM}\phi_{wt}}{\phi_{wt}\rho_{PSS-PCM} + (1-\phi_{wt})\rho_{np}} \tag{11}$$

5. Numerical approach, grid sensitivity analysis, and code verification

The enthalpy approach is employed to numerically simulate the SS-PCM phase change during the heat extraction from the electronic device. The discretization of governing equations is adopted by the finite element method (FEM), which is based on an unstructured triangular mesh to reconstitute the highly complex geometry of tree-shaped fins properly. Also, structured elements are used to discretize the enclosure's plate-fin structure. The commercial CFD package of COMSOL Multi-physics software was carefully employed to solve the governing equations perfectly. Therefore, the validity of the numerical findings has been checked first by the grid independence test.

The time evolution of the *IPF* during the heat extraction period characterizes the phase change performance of the heat sink. The grid

independence tests were done individually for plate and tree-shaped fins, as shown in Figs. 3 and 4. It can be concluded from grid independence tests that the grids with 2065 and 7805 elements are suitable for simulating the SS-PCM phase change process.

Moreover, the proposed mathematical model validation is checked with the experimental findings available in the literature. Ismail et al. [34] performed an experimental study of the PCM solidification around a vertically configured isothermal cylinder with axial fins. Initially, in their experiment, the PCM was entered under a superheated liquid state, 9.2 °C greater than the fusion temperature, and exposed to a cold cylinder where its inner wall temperature was reduced to be 36 °C lower than the phase-change temperature to launch the discharging process. Both experimental data [34] and numerical findings of the present model for the time variation of temperature distributions of the PCM domain are compared, as shown in Fig. 5. As illustrated, there is good agreement with the experimental data. As a result, the developed model can be used to explore the melting process during the heat extraction from a finned-enclosed concentrated heat source.

6. Results and discussion

The time evolution of the phase change contours of the SS-PCM is illustrated in Figs. 6 to 9. The impact of the fin material for a plate-fin structure is shown in Fig. 6 and for a tree-shaped structure in Fig. 7. For a plate-fin structure, SS-PCM starts the first stage of phase change in the bottom part of the enclosure. For Al and Cu, SS-PCM directly undergoes a phase change in the vicinity of the fins, while it remains limited to the bottom for steel 302. This is indeed related to the thermal conductivity of each material. Al and Cu are highly conductive, so heat is quickly transferred from the heat source through the fin, which is heated along its length. For steel 302, due to the low thermal conductivity, the heat transfer remains mainly concentrated in the zone neighboring the heat source. Carbon steel represents an intermediate behavior compared to the other materials. As time goes by, the same trend persists, and it can be seen that the phase change of SS-PCM is more uniform for Al and Cu as the phase change flow occurs in all the zones of the cavity, while it remains limited to the bottom half of the cavity for steel. In the final stage, almost all the SS-PCM in the cavity experiences the phase change for Al and Cu, and similar but to a lesser extent for carbon steel, while a fair amount of PCM remains in the regular solid phase in the upper part of the enclosure for steel 302. As for the tree structure, similar behavior is observed initially where the phase change of SS-PCM occurs in the vicinity of the fins. As time goes by, the SS-PCM phase change is more uniform and occurs in various locations in the cavity, even for steel. This is due to the shape of the tree structure, which covers different zones in the enclosure. On the negative hand, it can be seen in the last stage that not all SS-PCM undergoes phase change in the cavity, even in the case of Al and Cu, as some SS-PCM remains in the regular phase near the top wall.

This is due to the structure's height, which is lower than the plate-fin structure. On the other hand, a more uniform phase change is observed for the two steel materials compared to the plate-fin structure, due to the effect of the geometrical shape of the tree structure in the bottom half of the region, as the top part of both structures does not exhibit the phase change and is not therefore affected by the difference in height between the plate fin and tree structures.

The influence of the nanoparticle fraction, W_t on the phase change contours is illustrated in Figs. 8 and 9 for a plate-fin structure and a tree-shaped structure, respectively. As mentioned earlier, W_t has a very limited effect on the thermal behavior of the SS-PCM in the cavity. This can be validated by the contours of phase change, which are the same when W_t is changed from 0% to 3%, whether in the case of plate-fin or tree structure. This confirms that the heat transfer is dominated by the diffusion from the heat source through the fins to the SS-PCM.

Figs. 10 and 11 depict the variations of the normalized fraction of the phase change (*IPF*) and the power as functions of time for different fin materials in a plate-fin structure and a tree-shaped structure, respectively. In all cases, the *IPF* increases in a similar way for a short initial stage, less than 400 *s*, then increases rapidly until reaching full phase change in a second stage. The initial rate of increase is higher for a tree structure than for a plate-fin structure. However, in the final stage of phase change, the slope of the *IPF* curve gets lower in the case of a tree structure, indicating a reduced phase change rate during that period. So, overall, the phase change rate is initially higher for a tree structure compared to a plate one, but it gets lower in the final stage of phase change, such that full phase change is achieved faster in a plate-fin structure. Regarding the fin material, it can be seen in both cases of plate-fin and tree structures that the rate of phase change is the lowest for steel 302 compared to the other materials due to its relatively low thermal conductivity. On the other hand, the fastest phase change is achieved in the case of aluminum and copper, followed by carbon steel for a plate-fin structure. In fact, the full melting time is about 50% lower for Al and Cu compared to steel 302.

At the same time, all the three materials have similar phase change rates in the case of a tree structure, with a slight advantage for aluminum and copper, pointing out the contribution of such a structure to an

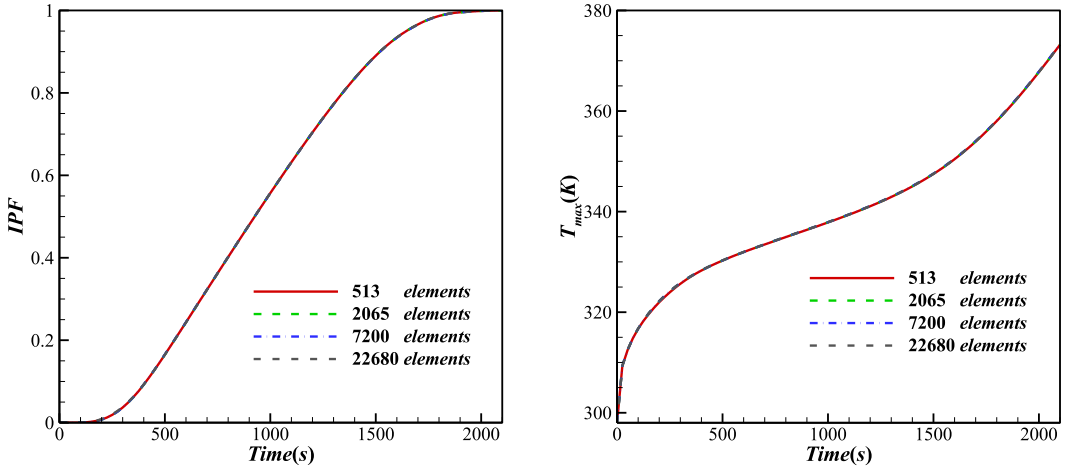

Fig. 3. Dependency of (a) *IPF* and (b) T_{max} on the mesh size for aluminum plate-fin structure at $W_t = 0$ % .

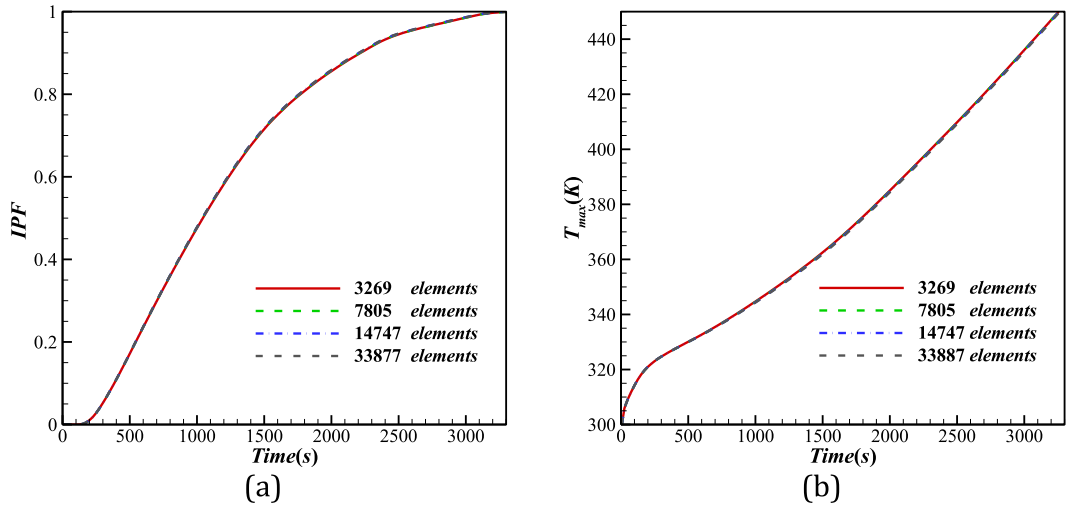

Fig. 4. Dependency of (a) *IPF* and (b) T_{max} on the mesh size for aluminum tree-shaped fin structure at $W_t = 0\%$.

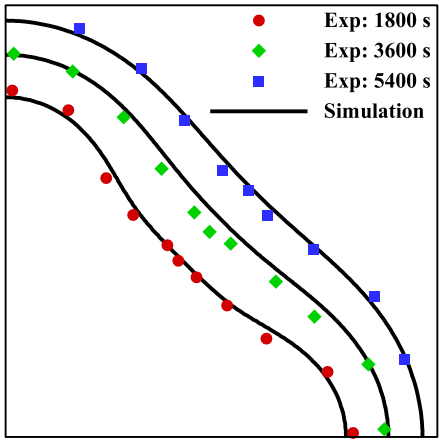

Fig. 5. Comparison between the phase change fields of the study addressed by Ismail et al. [34] and the current work.

optimized thermal distribution in the enclosure, reducing the impact of the material thermal conductivity. Here, Al and Cu are only about 25% faster in melting than steel 302. The power seems to be less influenced by the fin material, as the difference between its values is less than 1%. Despite the change in the phase change time, the energy storage, which is affected by the heat capacity of the fins, compensates for the difference such that the energy storage is similar in all cases.

The effect of the fin material on the variations of the maximum temperature T_{max} and the temperature non-uniformity parameter ΔT in a plate-fin structure as functions of time in the case of plate-fin and tree structures is shown, respectively, in Figs. 12 and 13. As the objective of the tree structure is to improve the heat diffusion from the heat source towards the SS-PCM, the study of these two parameters, T_{max} and ΔT, is very important as it indicates the efficiency of such diffusion. In all cases, the variation of T_{max} can be divided into two stages. In the initial short one, T_{max} rises substantially once the heat source is activated; then, in the second one, its variation slope decreases as the SS-PCM absorbs the heat and undergoes a phase change. The variation of ΔT follows a similar trend, and its variation is lower in the second stage. A relatively greater increase of T_{max} can be observed in the case of a tree structure. However, the value of ΔT is also lower for that structure, indicating a better heart diffusion and confirming the optimization of the enclosure by the presence of the tree structure. Concerning the material used, it is clear that in both structures, T_{max} and ΔT both have their highest values

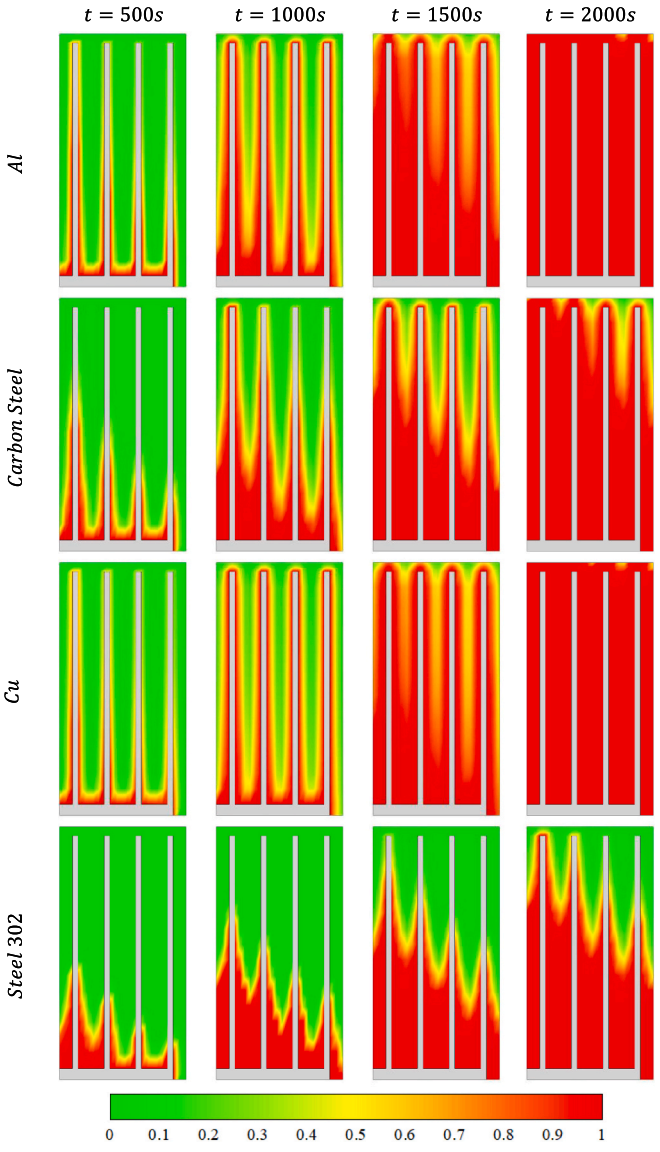

Fig. 6. Phase change contours of the branch fin configuration for different materials of fins at $W_t = 0.0\%$.

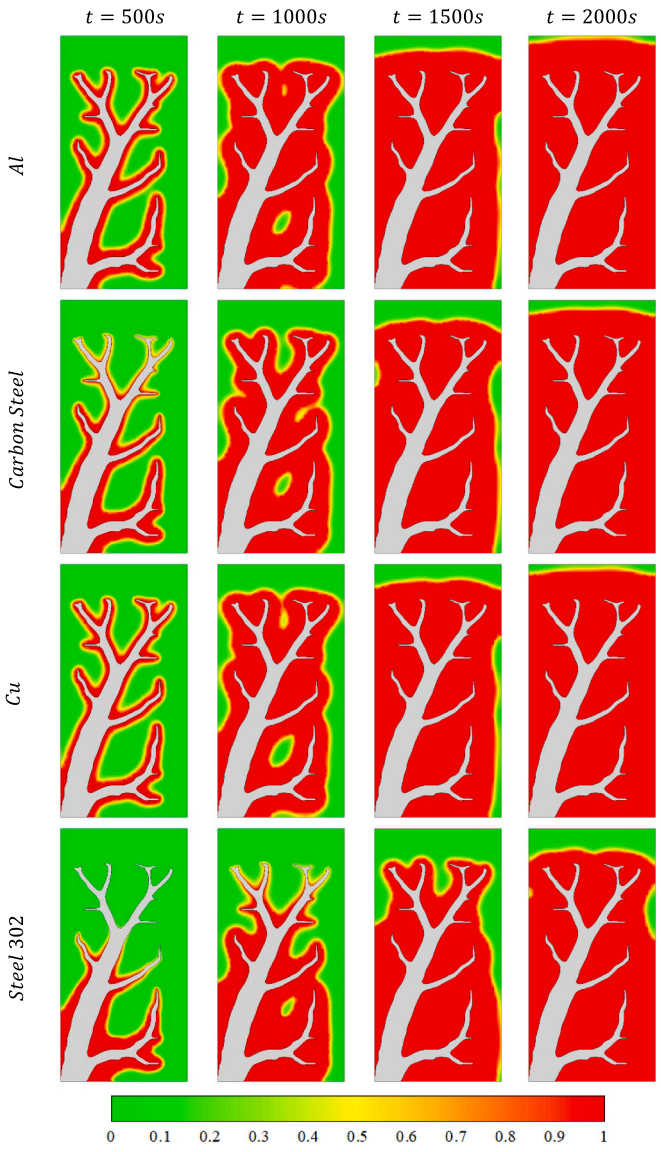

Fig. 7. Phase change contours of the tree fin configuration for different materials of fin at $W_t = 0.0\%$.

when steel 302 is used, which also corresponds to the lowest rate of SS-PCM phase change and consequently, the lowest heat diffusion. For instance, T_{max} is around 150% and 125% higher than Cu after 2500 s, in plate fins and tree structure, respectively. In both structure types, the best diffusion is achieved for copper and aluminum, and to a lesser extent, carbon steel, which corresponds to the phase change rate of each material.

Figs. 14 and 15 illustrate, respectively, the impact of the nanoparticle mass fraction, W_t on the time evolution of *IPF* and the power in a plate-fin structure. It is clear that varying W_t has a very limited effect on the two studied parameters. The increase of *IPF* is slightly slower for $W_t =$ 3%, but full phase change is reached at the same time for all the values of W_t. The same limited impact is observed for the power. In fact, less than 1% variation in the value of power is observed when varying W_t between 0% and 3%.

The variations of T_{max} and ΔT in a plate-fin structure as functions of time is plotted in Figs. 16 and 17, respectively. The overall variations of T_{max} and ΔT reveal again a minimal effect of W_t on their variation. Zooming on the last stage of melting shows less than 1% variation in both T_{max} and ΔT when W_t is varied between 0% and 3%.

In the case of a tree structure, the effects of the nanoparticle mass

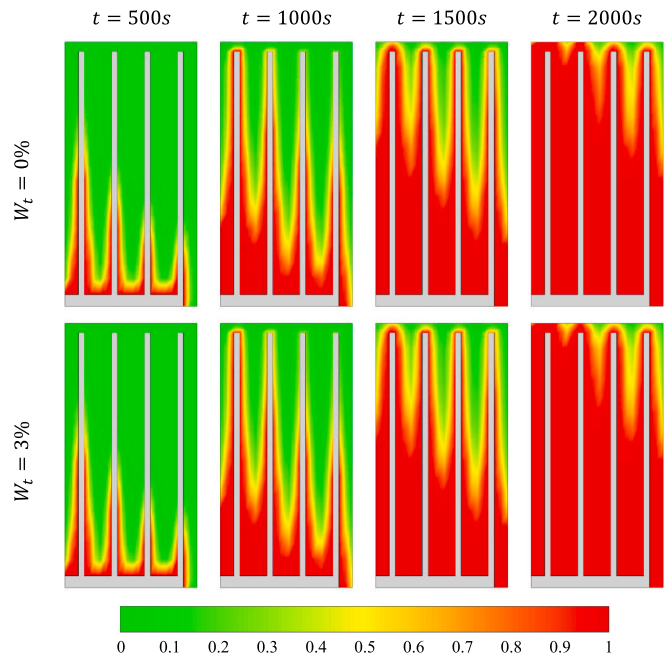

Fig. 8. Phase change contours of the branch fin configuration for different mass fraction.

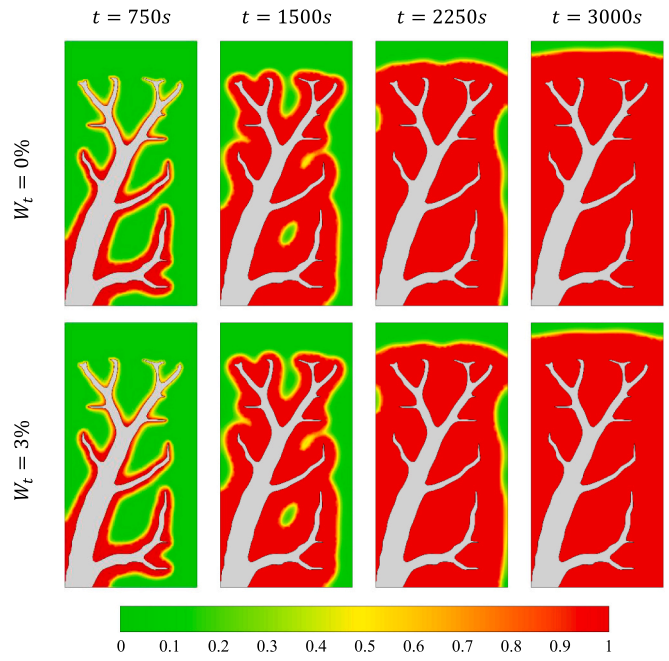

Fig. 9. Phase change contours of the tree fin configuration for different mass fraction.

fraction on the *IPF* and on the power are described in Figs. 18 to 19, and its effects on T_{max} and ΔT are depicted in Figs. 20 to 21. Similar to the results obtained in a plate-fin structure, the influence of W_t on the observed results is very limited. In fact, no difference at all is observed in the variation of *IPF*, while the difference in variation of the other parameters remains less than 1% when W_t is changed. Overall, changing the mass fraction of the nanoparticles seems to have a minimal impact on the thermal behavior of the enclosure in both structure types, which indicates that the heat transfer is largely affected by the presence of fins and is dominated by the heat diffusion from the fins to the SS-PCM that consequently undergoes the phase change.

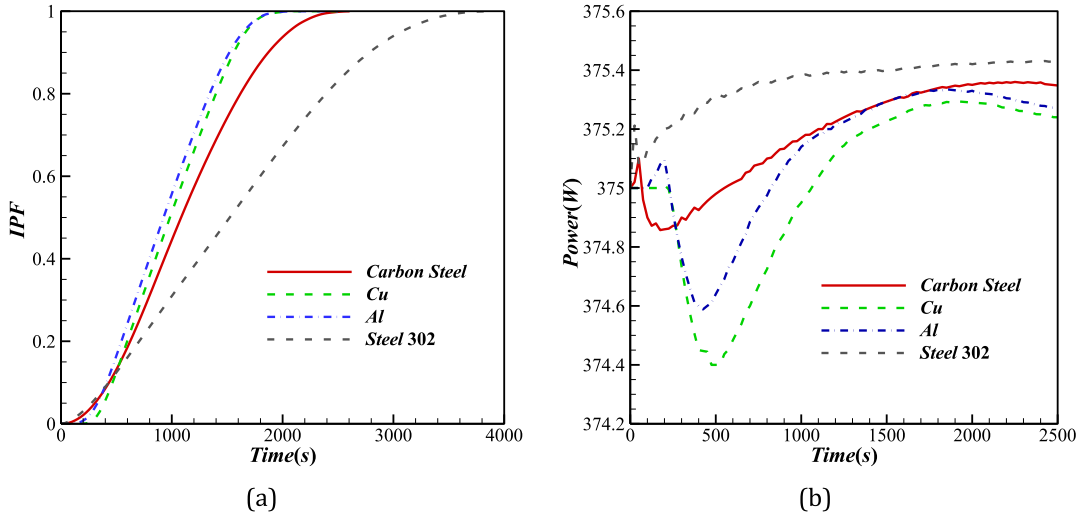

Fig. 10. The effect of fin material on (a) the *IPF* and (b) the power of heat sink with the plate structure fins at $W_t = 0\%$.

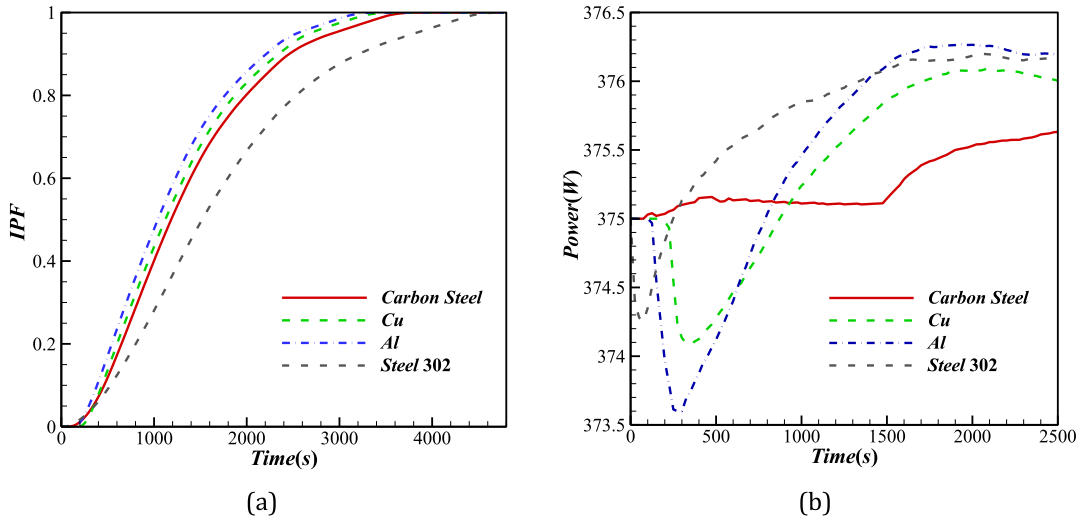

Fig. 11. The effect of fin material on (a) the *IPF* and (b) the power of heat sink of the tree-shaped structure fins at $W_t = 0\%$.

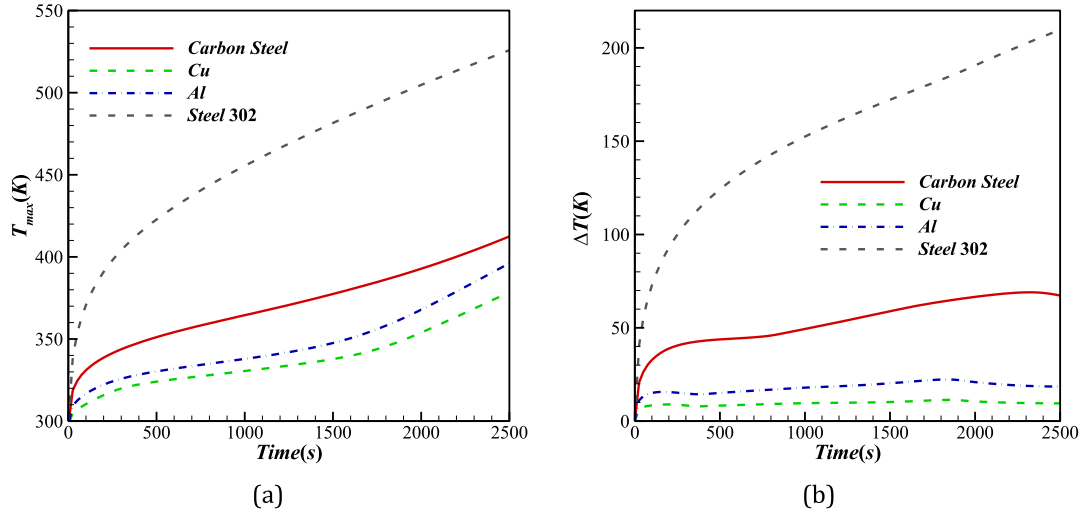

Fig. 12. The effect of fin material on (a) T_{max} and (b) ΔT of the heat sink with the plate structure fins at $W_t = 0\%$.

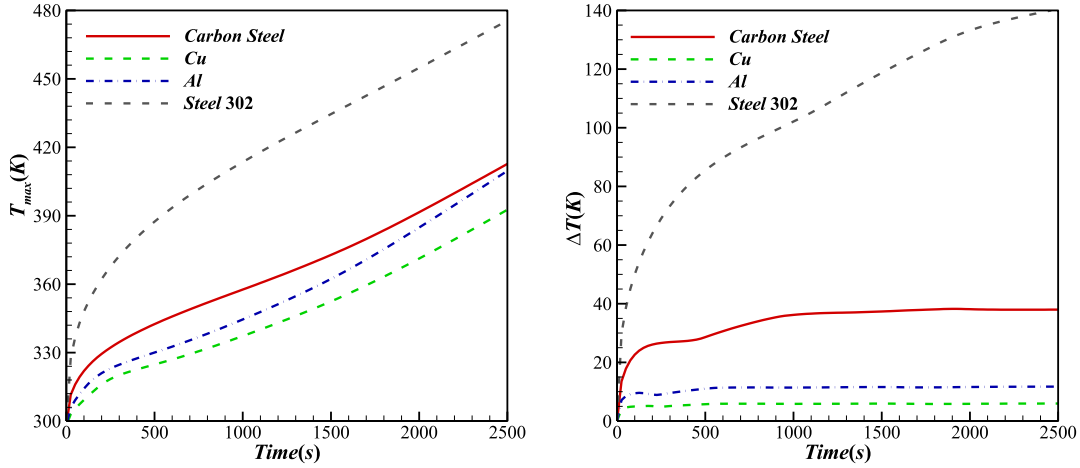

Fig. 13. The effect of fin material on (a) T_{max} and (b) ΔT of the heat sin with the tree-shaped fin structure at $W_t = 0\%$.

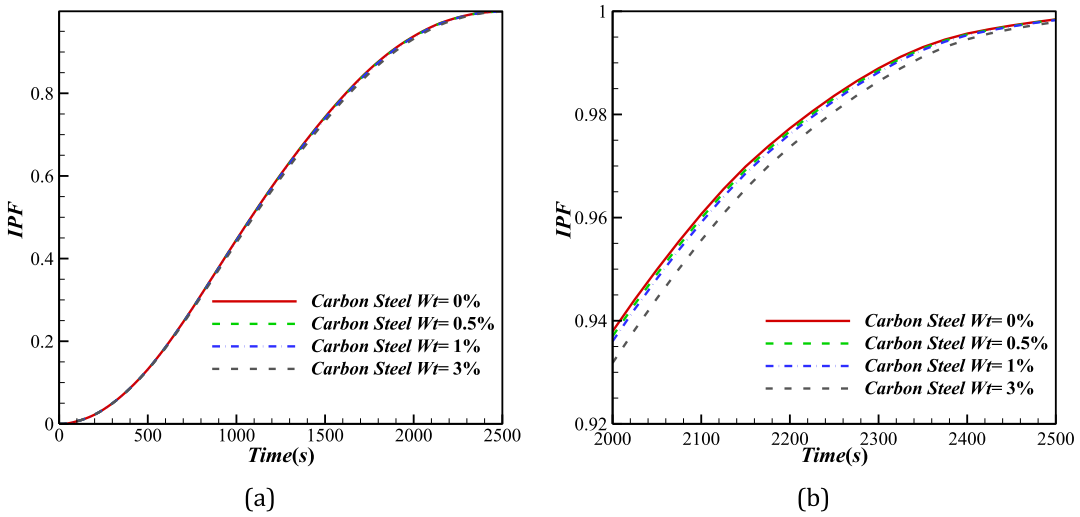

Fig. 14. The effect of mass fraction of nanoparticles on *IPF* for the plate fin structure.

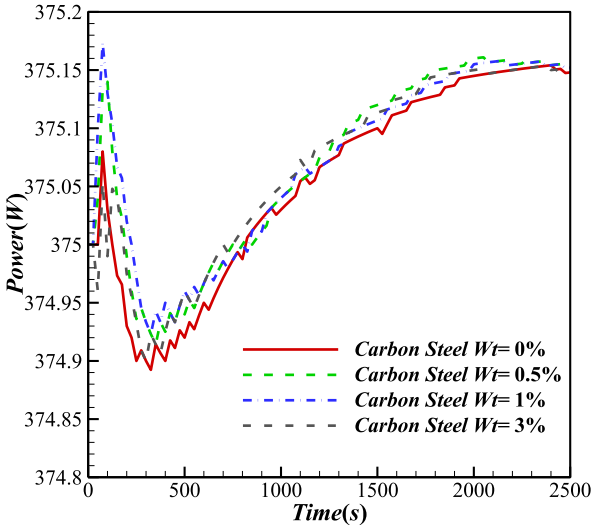

Fig. 15. The effect of mass fraction of nanoparticles on the power for the plate-fin structure.

Fig. 22 compares the *IPF* of a plate-fin structure and a tree-shaped fin structure for various fin materials. It is noted that the *IPF* is higher in a plate-fin structure compared to the tree-shaped fin structure for all the fin metals except for steel 302. As discussed in Figs. 6 and 7, heat is transmitted faster in highly conductive fins. The height of the fins in the plate-fin structure is larger than the one in the tree-shaped fin structure, so heat is transmitted to the SS-PCM in the top and bottom parts of the enclosure. On the other hand, for steel 302, the thermal conductivity is low, and heat is transmitted slowly through the fin. The larger height of the plate-fin structure does not play a role in heat transfer to the SS-PCM in the upper part of the cavity.

The power of a plate-fin structure and a tree-shaped fin structure is compared in Fig. 23 for different materials. It can be seen that in all cases, the power of the heat sink with the tree-shaped fin structure ends up being higher than the plate-fin structure. However, the change between the two is negligible, as less than 1% variation can be observed between them at various times. This is due to the fact that the latent heat changes when the SS-PCM phase change rate varies between the two structure types; it is recovered by the amount of sensible heat during heat diffusion as well as the heat stored in the structure fins.

The values of ΔT and T_{max} in the plate-fin structure and the tree-shaped fin structure are depicted respectively in Figs. 24 and 25. It is

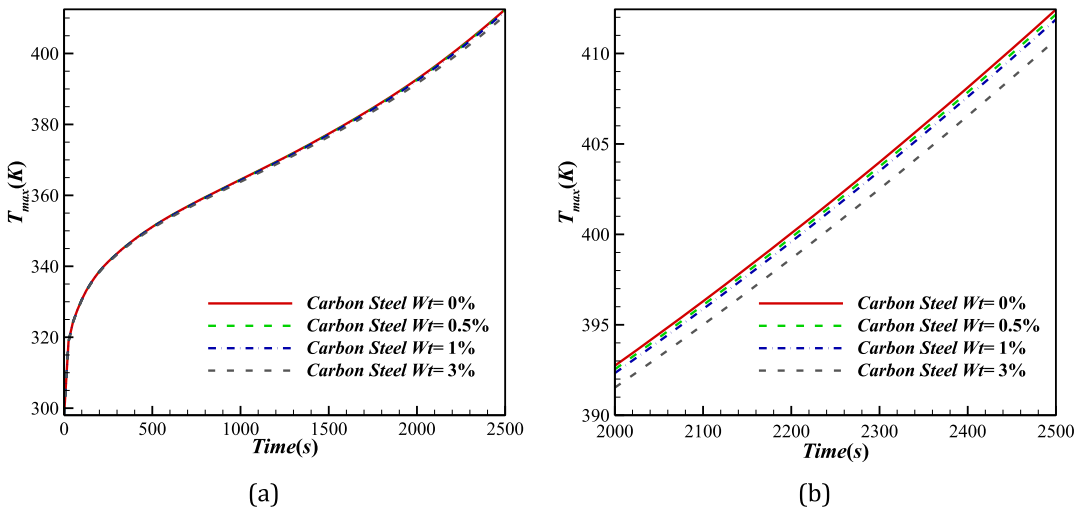

Fig. 16. The effect of mass fraction of nanoparticles on T_{max} for the plate fin structure.

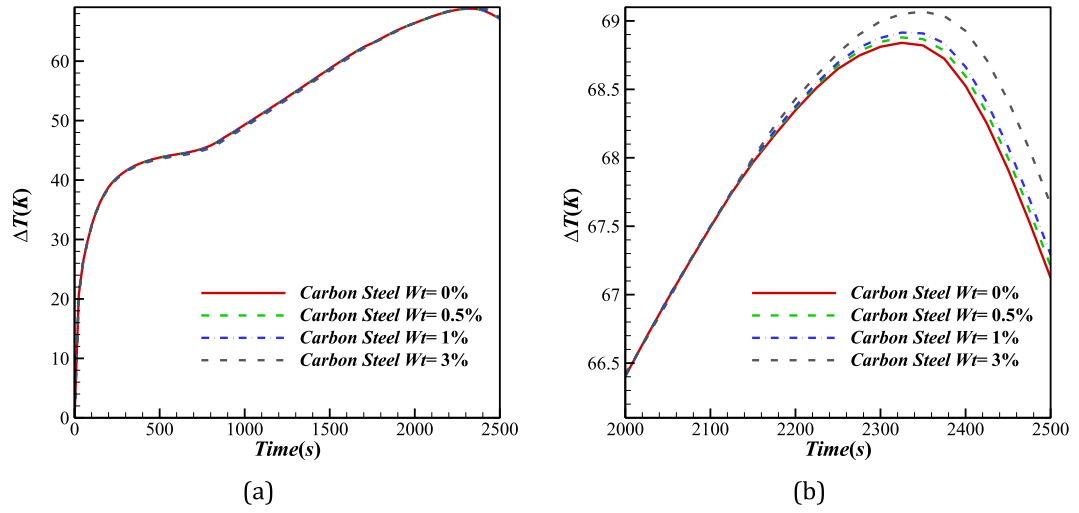

Fig. 17. The effect of mass fraction of nanoparticles on ΔT for the plate fin structure.

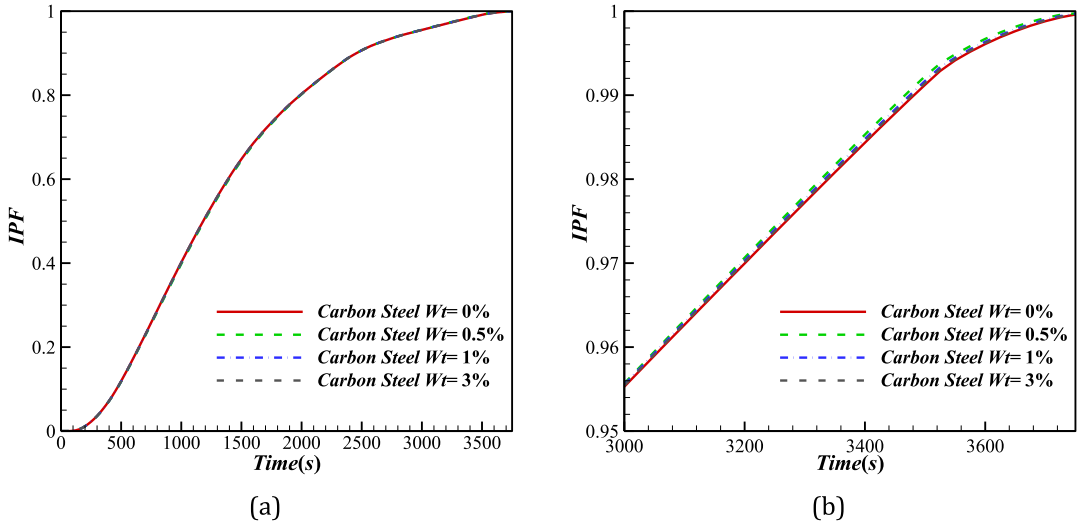

Fig. 18. The effect of mass fraction of nanoparticles on *IPF* for the tree-shaped fin structure.

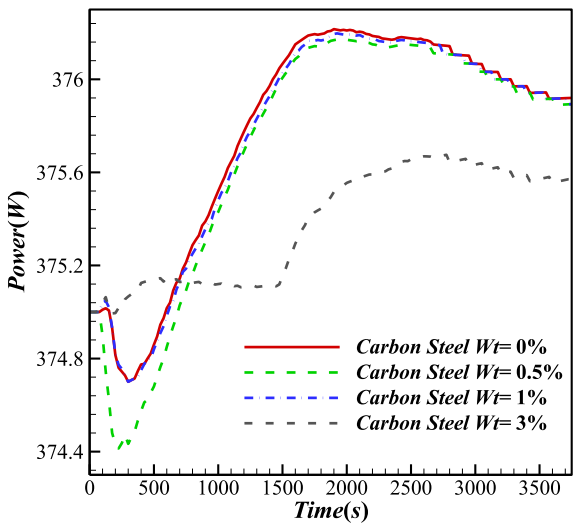

Fig. 19. The effect of mass fraction of nanoparticles on the power for the tree-shaped fin structure.

shown the value of T_{max} at the various times is highest for steel 302, as SS-PCM phase change is at its lowest in that case and heat transfer from the heat source is reduced. In the figre, at 2000 s, T_{max} for steel 302 is 135% higher than Cu in flat plates, and 120% in tree structure. In addition, T_{max} is higher in the tree-shaped fin structure than the plate-fin one for all the metals except for steel 302, which is related to the variation of *IPF* as discussed in Fig. 11. On the other hand, ΔT is lower in the tree-shaped fin structure compared to the plate-fin structure for all the metals. It is, respectively, 50%, 55%, 32% and 55% lower for Cu, carbon steel, steel 302 and Al at 2000 s. This validates the optimization of heat diffusion by the geometry by reducing the temperature difference on the fins.

7. Summary

The main results of the present study can be summarized as:

- The melting of PCM is intensified when materials with higher thermal conductivity are used in both the plate-fin and tree structures. Aluminum and copper showed the highest melting rates compared to the other tested materials. Full melting in Al and Cu is achieved 50%

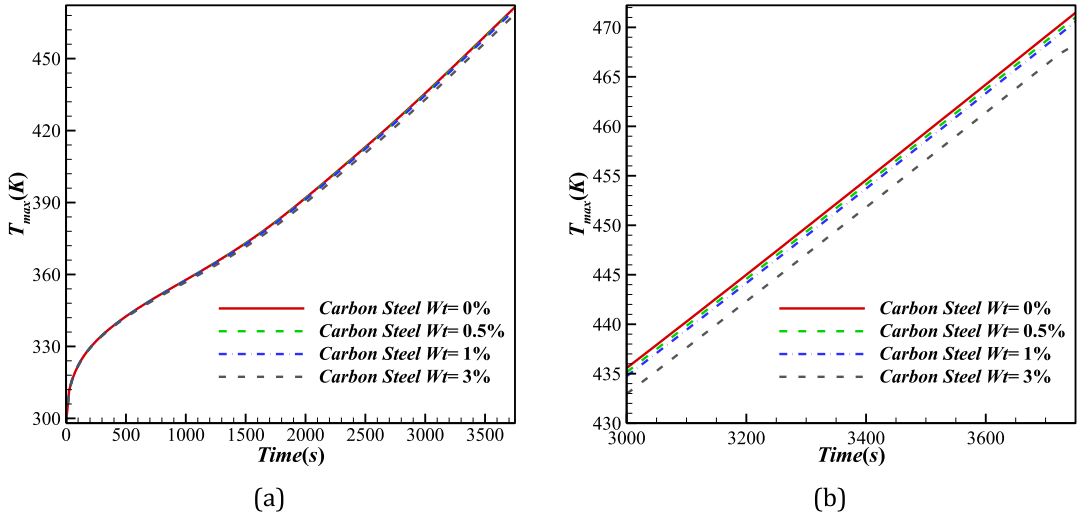

Fig. 20. The effect of mass fraction of nanoparticles on T_{max} for the tree-shaped fin structure.

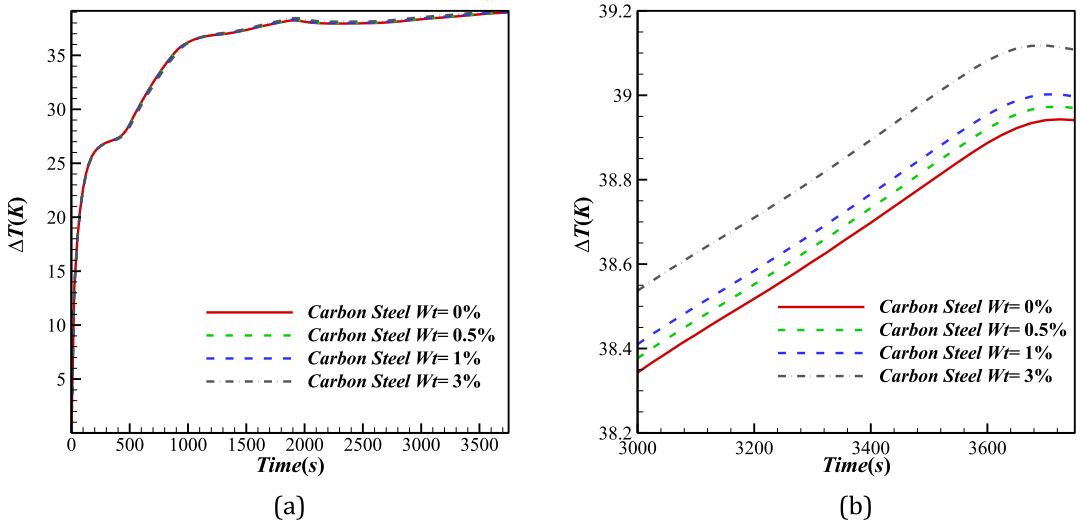

Fig. 21. The effect of mass fraction of nanoparticles on ΔT for the tree-shaped fin structure.

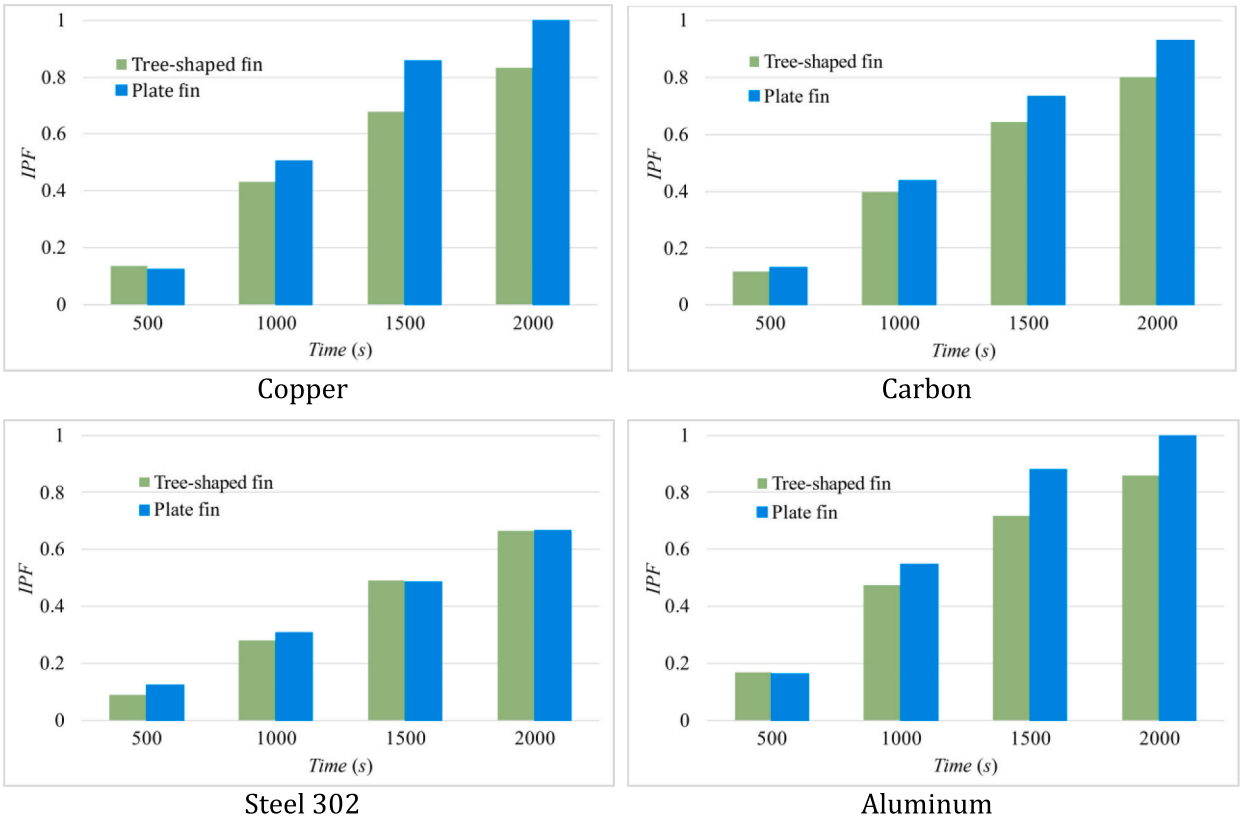

Fig. 22. Comparison between the fraction of irregular solid phase for the tree-shaped fin and plate-fin structures with different materials.

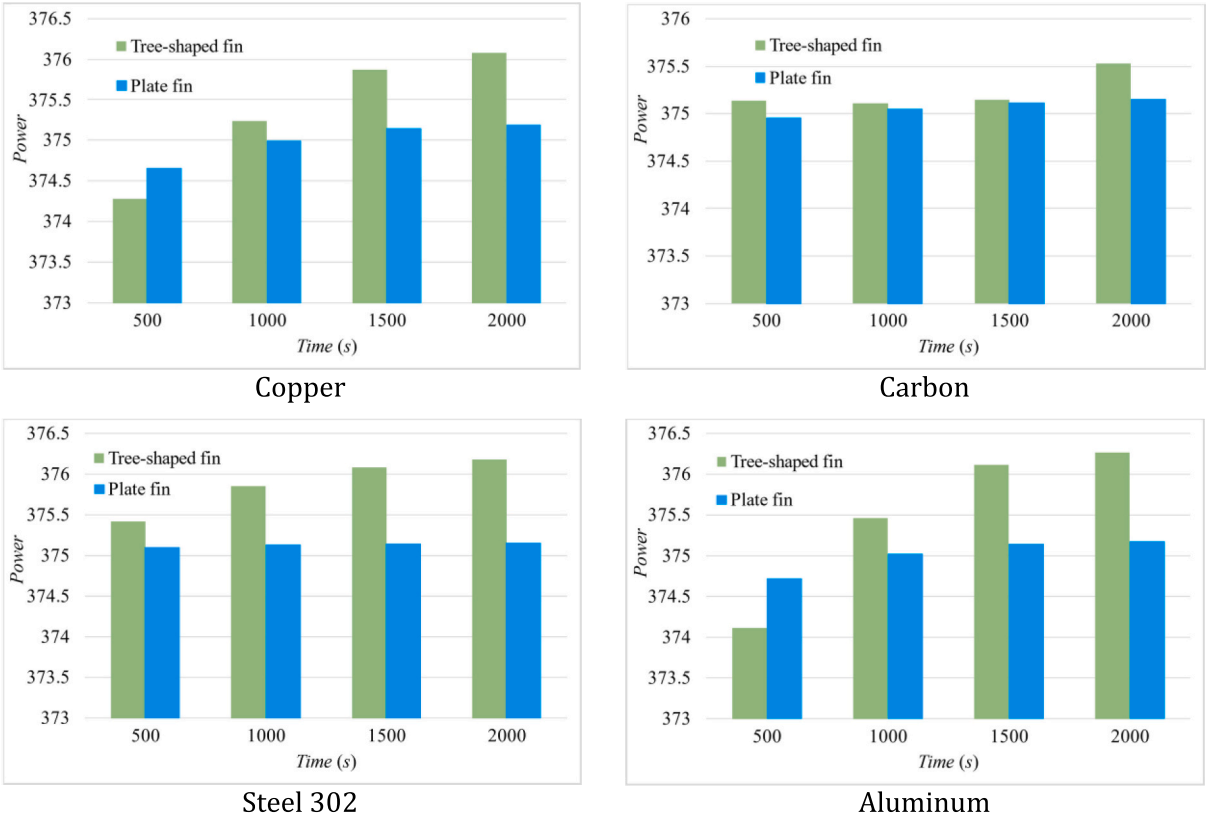

Fig. 23. Comparison between the power of heat sink with the tree-shaped fin and plate-fin structures with different materials.

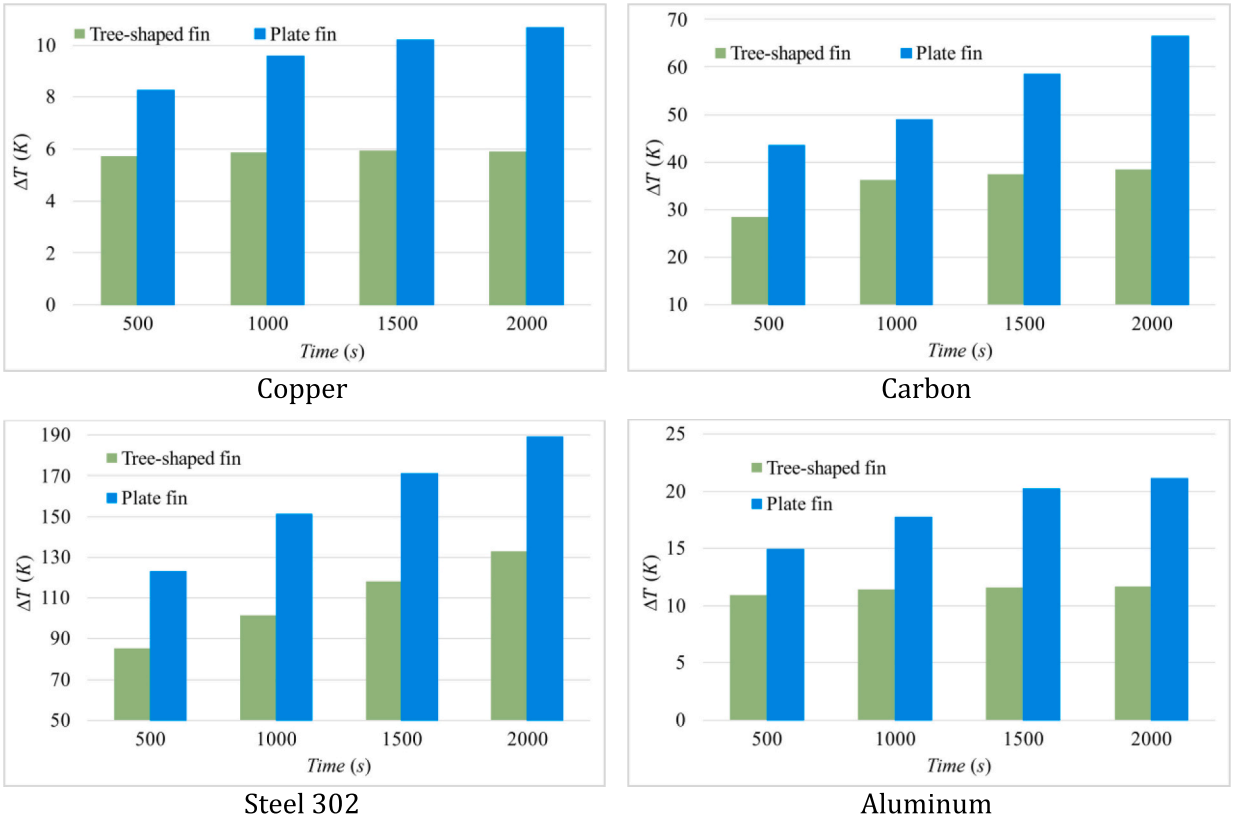

Fig. 24. Comparison between the temperature non-uniformity of the tree-shaped fin and plate-fin structures for different materials of fins.

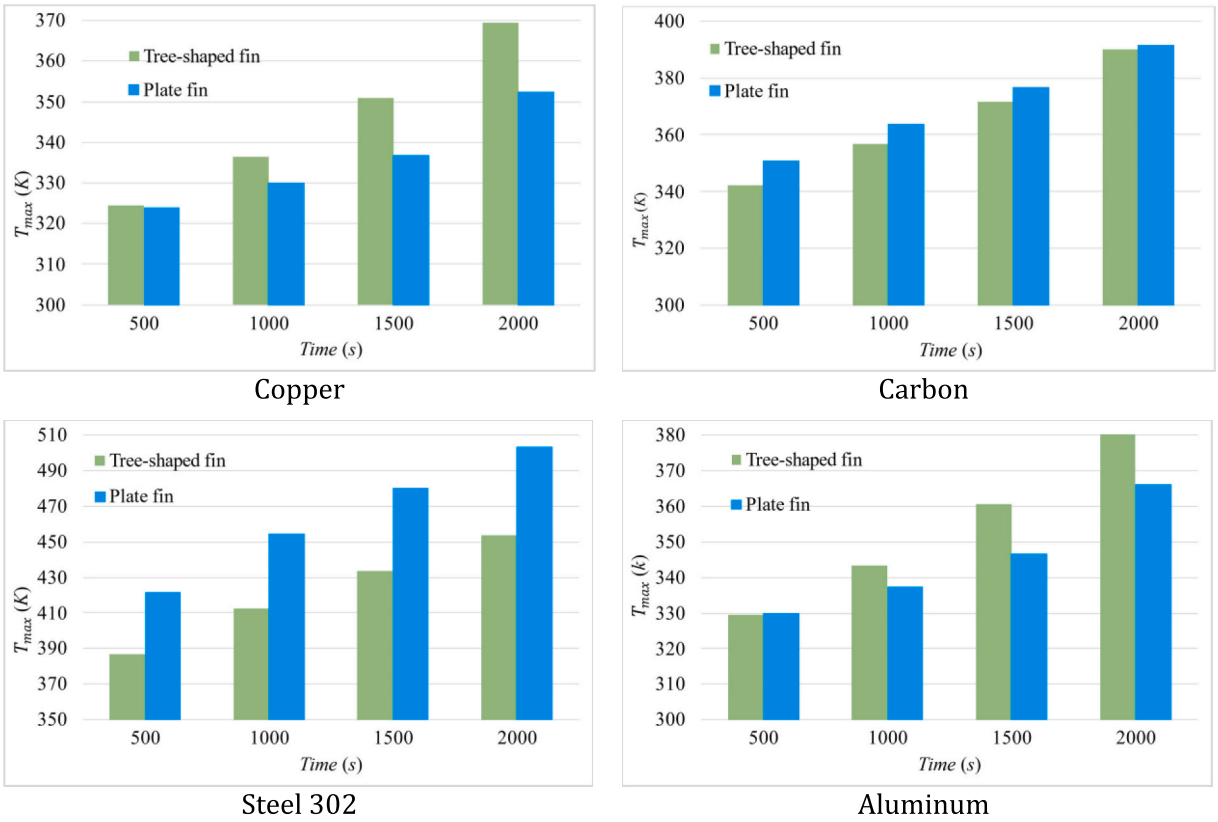

Fig. 25. Comparison between the maximum temperature of the tree-shaped fin and plate-fin structures for different materials of fins.

and 25% faster than steel 302 in flat plates and tree structure, respectively.

- A tree structure improves the heat diffusion from the heat source towards the PCM. However, it seems that the height of the structure plays an important role in transferring the heat towards the PCM in the upper part of the enclosure, mainly for highly conductive materials. In the present study, the height of the plate-fin structure was greater than the tree structure, and faster PCM melting was achieved in the former one for Al and Cu. For materials with lower thermal conductivity, heat transfer is optimized in the case of a tree structure, as heat transfer is already limited in the upper part of the cavity. The maximum temperature is 5% higher in the case of tree structure compared to flat plates for Al and Cu, while it is 10% and 1% lower in flat plates for steel 302 and carbons steel, respectively. In order to have an overall optimization for all the materials, the tree structure can be designed with the same height as the plate-fin cavity.
- The effect of nanoparticle mass fraction on the thermal behavior of the PCM in the enclosure is very limited. Less than 1% difference was observed in metling rate and cavity temperature when the nanoparticle fraction was varied. Heat transfer is substantially more affected by the fins and is dominated by the heat diffusion through the fin structure towards the PCM that undergoes melting.

CRediT authorship contribution statement

Nidhal Ben Khedher: Conceptualization, Software, Methodology, Writing – original draft, Writing – review & editing. **Mohammad Ghalambaz:** Methodology, Writing – original draft. **Abed Saif Alghawli:** Conceptualization, Methodology, Formal analysis, Data curation. **Ahmad Hajjar:** Conceptualization, Investigation, Writing – original draft, Writing – review & editing. **Mikhail Sheremet:** Conceptualization, Writing – original draft, Writing – review & editing. **S.A.M. Mehryan:** Supervision, Investigation, Writing – original draft, Methodology, Writing – review & editing.

Declaration of Competing Interest

The authors declare that they have no conflict of interest.

Acknowledgements

This research of Mohammad Ghalambaz and Mikhail Sheremet was supported by the Tomsk State University Development Programme (Priority-2030).

References

[1] W. Hua, L. Zhang, X. Zhang, Research on passive cooling of electronic chips based on PCM: a review, J. Mol. Liq. 340 (2021) 117183.
[2] J. Mathew, S. Krishnan, A review on transient thermal management of electronic devices, J. Electron. Packag. 144 (1) (2022).
[3] A. Arshad, M.I. Alabdullatif, M. Jabbal, Y. Yan, Towards the thermal management of electronic devices: a parametric investigation of finned heat sink filled with PCM, Int. Commun. Heat Mass Transf. 129 (2021) 105643.
[4] R. Kalbasi, Introducing a novel heat sink comprising PCM and air-adapted to electronic device thermal management, Int. J. Heat Mass Transf. 169 (2021) 120914.
[5] M. Ghalambaz, J. Zhang, Conjugate solid-liquid phase change heat transfer in heatsink filled with phase change material-metal foam, Int. J. Heat Mass Transf. 146 (2020) 118832, 2020/01/01/, https://doi.org/10.1016/j.ijheatmasstransfer.2019.118832.
[6] S. Xu, C. Zhou, C. Xu, Composite Heat Dissipation Device Adopting Composite Phase Change Material and micro-Channel Liquid Cooling, China, 2020.
[7] D. Cheng, et al., Heat Dissipation Device Based on Combination of PCM Fin Heat Pipe Integrated Plate and Semiconductor Refrigeration Piece and Implementation Method Thereof, China, 2020.
[8] X. Su, F. Lai, D. Yan, Method for Pouring Phase-Change Material of Phase-Change Temperature Control Component of Electronic Device, China, 2020.
[9] Y. Zhao, J. Qiu, L. Sun, Passive Phase-Change Material Temperature Regulating System of Power Battery, China, 2020.
[10] M. Teggar, et al., A comprehensive review of micro/nano enhanced phase change materials, J. Therm. Anal. Calorim. (2021) 1–28.
[11] J.D. Williams, G. Peterson, A review of thermal property enhancements of low-temperature nano-enhanced phase change materials, Nanomaterials 11 (10) (2021) 2578.
[12] F.T. Najim, et al., Improved melting of latent heat storage using fin arrays with non-uniform dimensions and distinct patterns, Nanomaterials 12 (3) (2022) 403.
[13] K. Chen, H.I. Mohammed, J.M. Mahdi, A. Rahbari, A. Cairns, P. Talebizadehsardari, Effects of non-uniform fin arrangement and size on the thermal response of a vertical latent heat triple-tube heat exchanger, J. Energy Stor. 45 (2022) 103723.
[14] K. Hosseinzadeh, et al., Effect of two different fins (longitudinal-tree like) and hybrid nano-particles (MoS2-TiO2) on solidification process in triplex latent heat thermal energy storage system, Alexandr. Eng. J. 60 (1) (2021) 1967–1979.
[15] P. Talebizadehsardari, et al., Effect of airflow channel arrangement on the discharge of a composite metal foam-phase change material heat exchanger, Int. J. Energy Res. 45 (2) (2021) 2593–2609.
[16] H.M. Ali, M.M. Janjua, U. Sajjad, W.-M. Yan, A critical review on heat transfer augmentation of phase change materials embedded with porous materials/foams, Int. J. Heat Mass Transf. 135 (2019) 649–673.
[17] M.E. Moghaddam, M.H.S. Abandani, K. Hosseinzadeh, M.B. Shafii, D. Ganji, Metal foam and fin implementation into a triple concentric tube heat exchanger over melting evolution, Theor. Appl. Mech. Lett. (2022) 100332.
[18] N.S. Bondareva, B. Buonomo, O. Manca, M.A. Sheremet, Heat transfer performance of the finned nano-enhanced phase change material system under the inclination influence, Int. J. Heat Mass Transf. 135 (2019) 1063–1072.
[19] K. Hosseinzadeh, E. Montazer, M.B. Shafii, A. Ganji, Solidification enhancement in triplex thermal energy storage system via triplets fins configuration and hybrid nanoparticles, J. Energy Stor. 34 (2021) 102177.
[20] K. Hosseinzadeh, M.E. Moghaddam, A. Asadi, A. Mogharrebi, D. Ganji, Effect of internal fins along with hybrid nano-particles on solid process in star shape triplex latent heat thermal energy storage system by numerical simulation, Renew. Energy 154 (2020) 497–507.
[21] C. Ho, C.-R. Siao, T.-F. Yang, B.-L. Chen, S. Rashidi, W.-M. Yan, An investigation on the thermal energy storage in an enclosure packed with micro-encapsulated phase change material, Case Stud. Therm. Eng. 25 (2021) 100987.
[22] M.R. Singh, A. Giri, A comparison of the performance of constant and dual height pin fins in phase change material cooling technique, J. Therm. Sci. Eng. Appl. 13 (4) (2021).
[23] S.H. Kim, C.S. Heu, J.Y. Mok, S.-W. Kang, D.R. Kim, Enhanced thermal performance of phase change material-integrated fin-type heat sinks for high power electronics cooling, Int. J. Heat Mass Transf. 184 (2022) 122257.
[24] M. Nakhchi, M. Hatami, M. Rahmati, A numerical study on the effects of nanoparticles and stair fins on performance improvement of phase change thermal energy storages, Energy 215 (2021) 119112.
[25] J. Xie, H.M. Lee, J. Xiang, Numerical study of thermally optimized metal structures in a phase change material (PCM) enclosure, Appl. Therm. Eng. 148 (2019) 825–837.
[26] K. Liu, A. Tovar, An efficient 3D topology optimization code written in Matlab, Struct. Multidiscip. Optim. 50 (6) (2014) 1175–1196.
[27] J. Xie, K.F. Choo, J. Xiang, H.M. Lee, Characterization of natural convection in a PCM-based heat sink with novel conductive structures, Int. Commun. Heat Mass Transf. 108 (2019) 104306.
[28] A. Fallahi, G. Guldentops, M. Tao, S. Granados-Focil, S. Van Dessel, Review on solid-solid phase change materials for thermal energy storage: molecular structure and thermal properties, Appl. Therm. Eng. 127 (2017) 1427–1441.
[29] C.R. Raj, S. Suresh, R. Bhavsar, V.K. Singh, Recent developments in thermo-physical property enhancement and applications of solid solid phase change materials, J. Therm. Anal. Calorim. 139 (5) (2020) 3023–3049.
[30] B. Praveen, S. Suresh, Experimental study on heat transfer performance of neopentyl glycol/CuO composite solid-solid PCM in TES based heat sink, Eng. Sci. Technol. Int. J. 21 (5) (2018) 1086–1094.
[31] X. Du, J. Qiu, S. Deng, Z. Du, X. Cheng, H. Wang, Flame-retardant and solid-solid phase change composites based on dopamine-decorated BP nanosheets/polyurethane for efficient solar-to-thermal energy storage, Renew. Energy 164 (2021) 1–10.
[32] C.R. Raj, S. Suresh, R. Bhavsar, V.K. Singh, A.S. Reddy, A. Upadhyay, Manganese-based layered perovskite solid–solid phase change material: synthesis, characterization and thermal stability study, Mech. Mater. 135 (2019) 88–97.
[33] C.R. Raj, S. Suresh, R. Bhavsar, V.K. Singh, K.A. Govind, Influence of fin configurations in the heat transfer effectiveness of solid solid PCM based thermal control module for satellite avionics: numerical simulations, J. Energy Stor. 29 (2020) 101332.
[34] K. Ismail, C. Alves, M. Modesto, Numerical and experimental study on the solidification of PCM around a vertical axially finned isothermal cylinder, Appl. Therm. Eng. 21 (1) (2001) 53–77.